Synthesis of CoFe 2 O 4 nanocubes

Christine Leroux, Fernandes de Medeiros, V. Madigou, A.L. Lopes-Moriyama, C. Pereira de Souza, Ch. Leroux

Synthesis of $CoFe_2O_4$ nanocubes

I. A. Fernandes de Medeiros[a,b], V. Madigou[a], A.L.Lopes-Moriyama[b], C.Pereira de Souza[b], Ch. Leroux[a,*]

[a] *Université de Toulon, AMU, CNRS, IM2NP, CS 60584, Toulon, F- 83041, France,*

[b] *Universidade do Rio Grande do Norte, DEQ/PPGEQ-LMNRC, Campus Universitário, Lagoa Nova 59072-970 Natal, Brazil*

*corresponding author : leroux@univ-tln.fr

Declarations of interest : none

ABSTRACT

Nanocubes of cobalt ferrite with stoichiometric composition, 20 nm in size, were obtained by a solvothermal route, with acetylacetonates precursors and benzyl alcohol as a solvent, in presence of oleylamine and a mixture oleic acid/oleylamine. The cobalt ferrites were characterized by X-ray diffraction and transmission electron microscopy coupled with energy dispersive spectroscopy. Synthesis parameters such as temperature, duration of the thermal treatment, concentration of precursors, were optimized.

keywords: cobalt ferrite, nanocubes, solvothermal, surfactant

INTRODUCTION

Ferrites are known for a long time for their magnetic properties along with good chemical stability under harsh environment. MFe_2O_4 compounds (M = metal 3d) are often biocompatible [1-3] and currently literature about ferrites nanoparticles is abundant, because of their potential in drugs delivery , in cancer curing through magnetic heating, or in medical imaging [4-8]. As nanoparticles, cobalt ferrite $Co_xFe_{3-x}O_4$ are superparamagnetic, or ferrimagnetic, depending on temperature of use and particle size [9-11]. In addition, these materials also have interesting catalytic and photocatalytic activity in various reactions, for applications in the field of water treatment [12-13] and gas sensing [14-15]. Creating composite materials based on $CoFe_2O_4$ nanoparticles can lead to new functional membranes; $CoFe_2O_4$ magnetostrictive nanoparticles were included in piezolectric polymers or dispersed in self-assembly of cellulose nanowhiskers in order to obtain magnetoelectric membranes [16-17]. Tuning the size, shape and composition of ferrite nanoparticles allows to tune their properties. Modifying the shape of magnetic nanocrystals modifies the surface anisotropy, hence is a key factor for tuning their magnetic properties, so attempts were done to synthesize various shape such as nanoplatelets [18], nanocubes [19], nanotubes and nanorods [20], and recently nanohexagons [21]. But it is in the domain of catalysis and gas sensing that many studies were conducted about the link between shapes and properties, leading to review papers [14,22].

Recently cobalt ferrites were investigated for their catalytic efficiency in various gas conversion [23-28]. The nanoparticles had no specific morphology, and the different behaviors were explained in terms of cation composition and particle sizes. The reactivity to gas of one given compound depends indeed on the surface/volume ratio, the porosity, the cation composition, but also on the exposed crystallographic facets [26]. Moreover, the shape of nanoparticles can be as fundamental as their size in determining the uniqueness and novelty of material properties [19,30].

In order to tailor the reactivity and catalytic properties of cobalt ferrites and to decorrelate the different influence on these properties, nano ferrites with different shapes, ie nanooctahedron [31,32] and nanocubes (this work) were synthesized. Cobalt ferrites are mixed ferrites, with an inversion degree that varies with the cobalt amount, particle size, and the synthesis method [33-

36], so the cation distribution, about the tetrahedral and octahedral sites, should also be taken into account when discussing cobalt ferrites properties [21].

Depending on the synthesis methods, the shape of nanoparticles is governed by the differences in surface energy, or by the differences in growth velocity of specific crystallographic facets. Surface energy considerations concern processes at thermal equilibrium, as facets growth velocity is linked to out of equilibrium processes [37]. For a face centered cubic structure (FCC), the surface energies of low Miller indices are ranked in the following order $\gamma\{1\ 1\ 1\} < \gamma\{1\ 0\ 0\} < \gamma\{1\ 1\ 0\}$. Thus, an octahedron, which is built by 8 {111} facets, is the equilibrium shape of a particle with an FCC structure. Out of equilibrium process synthesis can lead to out equilibrium crystals shapes, such as nanocubes, when the growth velocity of {111} outrank the one of {100} facets [37]. The growth velocity of facets, and thus the size and shape of particles, can be tailored by the use of specific surfactants[38-40].

The shape variation of cuboctahedron nanoparticles, limited by {111} and {100} facets, can be characterized by the ratio $r = \gamma\{1\ 0\ 0\}/\ \gamma\{1\ 1\ 1\}$, with $r = \sqrt{3}$ for an octahedron and $r = \sqrt{3}/2$ for a cube. Intermediate values correspond to cuboctahedron. The r ratio can be directly measured on images of [110] projected particles by measuring the h_{100}/h_{111}, h_{100} and h_{111} are the distances between two parallel {100} and {111} faces [41].

Many attempts were done to tailor the shape of nanoparticles, but mostly on noble metal particles [42-46]. Concerning cobalt ferrites, few $CoFe_2O_4$ particles with specific shapes such as nanooctahedron [31-32,47], core shell cubic shapes [48], mesoporous nanospheres [49], or nanocubes [50] are reported.

Recently, nanocubes of $Co_{0.6}Fe_{1.4}O_4$ have been synthesized from thermal decomposition of cobalt and iron organometallic precursors in long chain and high melting organic solvents in the presence of reducing agent and Oleic acid (OAc) and/or oleylamine (OAm) as surfactant [19,48,51-53]. However, either the obtained cobalt ferrite nanoparticles were cobalt deficient, or the composition of the nanoparticles was not controlled. This cobalt deficiency leads to the occurrence of Fe^{2+} in the cobalt ferrite, which in turn modify the catalytic and electrical properties compared to $CoFe_2O_4$ stoichiometric particles.

In this paper, for the first time, stoichiometric nanocubes of $CoFe_2O_4$ were synthesized from a single step solvothermal method, the benzyl alcohol route [54]. The benzyl alcohol route was already successfully used to obtain faceted cobalt ferrite with controlled composition, but with irregular shape [10,23]. OAm and/or OAc were added to the reaction medium and their effects on the composition and shape of the nanoparticles were investigated. In addition, for the nanoparticles produced with only OAm as surfactant, the synthesis parameters (temperature, reaction time, concentration of the precursors and concentration of OAm) on the nanoparticles shape were optimized.

MATERIALS AND METHODS

Materials

Iron (III) Acetylacetonate ($Fe(acac)_3$ 97%), Cobalt (II) Acetylacetonate ($Co(acac)_2$ 98%), benzyl alcohol (99,8 %), OAc (90%), OAm (70%), absolute ethanol (99,8%), acetone (99.5%) and dichloromethane (99.5%) were purchased from Alfa Aesar or Sigma-Aldrich and used in the synthesis reaction as received.

Synthesis of $CoFe_2O_4$ nanoparticles

Nanoparticles of cobalt ferrite were produced by the non-aqueous synthesis benzyl alcohol route [54] in the presence of different surfactants. In a typical synthesis, the surfactant was dissolved in 20 mL benzyl alcohol and then 1mmol of cobalt (II) acetylacetonate was added to the solution. The mixture was left under stirring for 2h for homogenization and, subsequently, 2 mmols of Iron (III) acetylacetonate were added. This corresponds to an acetylacetonate concentration of 0.15 M. The molar concentration of precursors was varied in this work between 0.08 M and 0.31M. As surfactant, OAc, OAm as well as an equimolar mixture of OAc/OAm, were used, with a molar concentration of 0.6 M, corresponding to a molar concentration ratio ([surfactant]: [$Fe(acac)_3$]) of 6. With OAm as surfactant, at an acetylacetonate molar concentration of 0.15M, the molar concentration of surfactant was varied from 0.4M to 0.75M.The mixture was then stirred for

another 2 h, transferred to a 45 ml teflon beaker, which was sealed in a steel autoclave and heated in an oven at 175 °C for 48 h. After the thermal treatment, in order to remove excess of solvent and surfactant, the suspension was diluted in absolute ethanol and centrifugated 3 times. Each time the supernatant was taken away, and alcohol was added. A final cycle of washing was done using dichloromethane and acetone in a 1:1 ratio. After washing, the powder was dried at 80 °C for 2 h. This way, one gram of powder was produced in one synthesis.

Thermal and chemical methods were applied to remove the residues of surfactants [55] and their efficiency tested using Fourier Transform InfraRed spectroscopy (FTIR). For thermal annealing two different treatment times were studied, namely 10h and 24h in air at 175 °C. Concerning the chemical washing the nanoparticle powders were purified using a mixture of acetic acid and acetone or using pure acetic acid. When the mixture was used, the nanoparticles were washed with 100 mL of solution acetic acid/acetone with volumetric ratio of 1:3, then centrifugated and washed with absolute ethanol. When pure acetic was used, the nanoparticles were dispersed in pure acetic acid by vigorous stirring at 80 °C for 10h, and then collected by adding ethanol followed by centrifugation.

Figure 1 shows the FTIR spectra obtained on a $CoFe_2O_4$ powder synthesized with OAm, before and after different purification treatments.

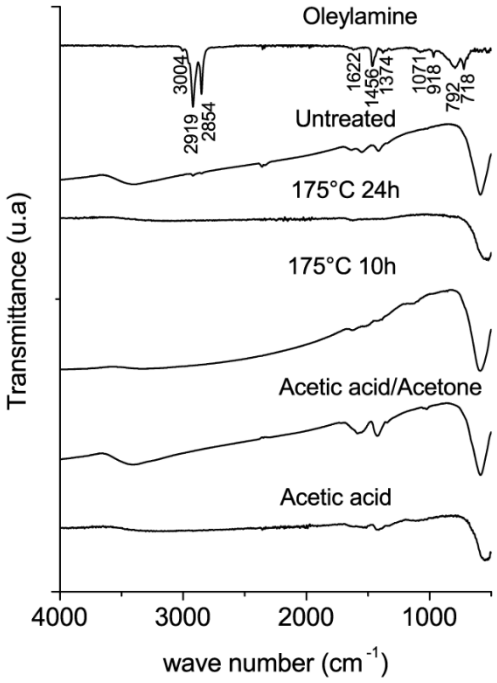

Figure 1: FTIR spectra of $CoFe_2O_4$ powders synthesized with OAm, before and after different purification methods. The FTIR spectrum of pure oleylamine is reported as a reference.

The FTIR spectrum of the $CoFe_2O_4$ nanoparticles without purification presents absorption bands around 1330-1650 cm^{-1}, 2919 cm^{-1} and 2854 cm^{-1}, which correspond respectively to the flexion modes of the $-NH_2$ group, methyl groups and to the stretching modes of CH bonds. The presence of these bands confirms the existence of OAm at the surface of the nanoparticles [56], so from Fig.1 on can conclude that chemical washing was not efficient. None of the energy bands related to the OAm molecule is observed in the IR spectrum of the heated nanoparticles at 175ºC for 24h, which proves the removal of the surfactant from the nanoparticles. On the other hand, the IR spectra of the nanoparticles heated at 175 °C for 10 h or submitted to chemical washing reveal residual peaks around 1330-1650 cm^{-1}. The presence of these bands and absence of energy bands around 2919 cm^{-1} and 2854 cm^{-1} indicates the breakage of the OAm molecule and its transformation into a smaller amine. Therefore, among the methodologies used, the heat treatment at 175 °C for 24 hours is the most effective treatment for obtaining OAm-free nanoparticles.

Characterization

X-ray diffraction (XRD) patterns of the powders were recorded on an Empyrean diffractometer (Panalytical) equipped with a CuK_α radiation source (λ = 0.15406 nm). Each sample was continuously scanned in a θ-2θ mode from 25 to 65° with a step of 0.007° and a scan speed of 0.002°/s. Morphologies, crystal sizes and chemical composition of the nanoparticles were determined by transmission electron microscopy (TEM), coupled with energy dispersive spectroscopy (EDS), using a Tecnai G2 200 kV with a LaB_6 source. The statistical study on particle size was carried on over 200 particles for each powder. For each sample, at least 20 EDS

analyses were performed at different scales to insure reliable statistical results. FTIR spectra were recorded in the wave number range 4000-500 cm^{-1} using a Bruker-Tensor 27 spectrometer.

RESULTS AND DISCUSSIONS

Influence of the nature of the surfactant on the chemical purity and shape of $CoFe_2O_4$ particles

Figure 2 shows the XRD patterns of the cobalt ferrite nanoparticles synthesized with OAm, OAc or a mixture OAc/OAm as surfactants. The XRD patterns of the nanoparticles confirm the formation of the cubic spinel structure with the space group Fd-3m, in accordance with the standard ICDD 22-1086, for the different powders. No additional peaks were present in the XRD patterns, indicating single phased powders.

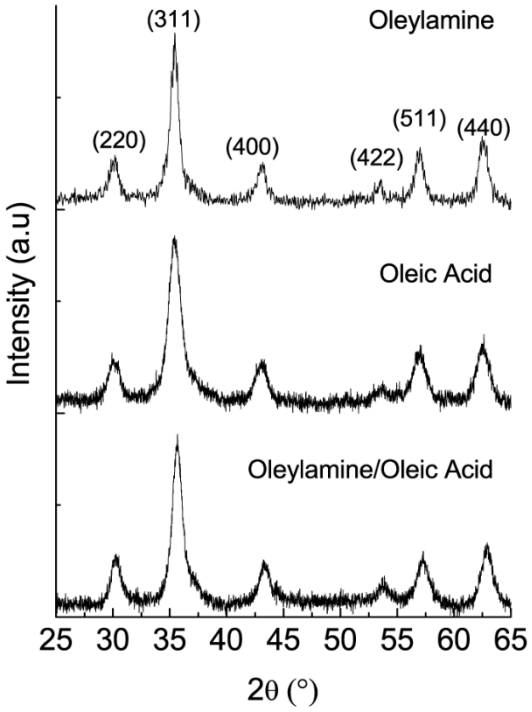

Figure 2 – XRD patterns of $CoFe_2O_4$ synthesized with different surfactants.

The TEM analysis coupled with EDS confirmed that the powders were single phased, each particle being monocrystalline, and showed the homogeneity of their chemical composition (Table

1). The nanoparticles synthesized only with OAm and OAc as surfactant have an atomic percentage of iron and cobalt corresponding to the stoichiometric composition $CoFe_2O_4$. On the other hand, the powder prepared with the OAc/ OAm mixture has a chemical composition of $Co_{0.6}Fe_{2.4}O_4$, thus is deficient in cobalt. Co-deficient cobalt ferrite are synthesized in reducing reaction medium where the Fe (III) ions are partially reduced to Fe (II) replacing Co(II) in the formation of ferrites [57].

Table 1 - Mean composition with the standard deviation σ, obtained by EDS analyses.

Surfactant	at.% Co	at. %Fe	Co/Fe	σ	Chemical formula
OAm	33	67	0.49	0.01	$CoFe_2O_4$
OAc	35	65	0.54	0.02	$Co_{1.05}Fe_{1.95}O_4$
OAc/ OAm	22	78	0.28	0.01	$Co_{0.6}Fe_{2.4}O_4$

The amine and carboxylic acid functional groups present in OAm and OAc may act as reducing agents, and they are more reductive when used together in an mixture than when they are used separately [58]. Cobalt-deficient cobalt ferrite nanoparticles have also been obtained by thermal decomposition of acetylacetonates with an OAc/ OAm mixture [57,59].Thus, one can conclude that the cobalt deficiency in the ferrite is due to a too reductive reaction medium, leading to the formation of ferrous ions.

Figure 3 shows the TEM images and particle size distributions of the nanoparticles produced with OAm (Fig.3a), OAc (Fig.3b) and OAc/ OAm (Fig.3c) as surfactants. Monodisperse nanoparticles were obtained in the presence of the different surfactants, but the type of surfactant influences the morphology and the size distribution of the nanoparticles. A powder consisting of two populations with distinct sizes was obtained in the presence of OAm. We observe clearly in the TEM image (Fig.3a) the presence of nanocubes around 20nm in size and smaller facetted particles, some of them having also a cubic shape.

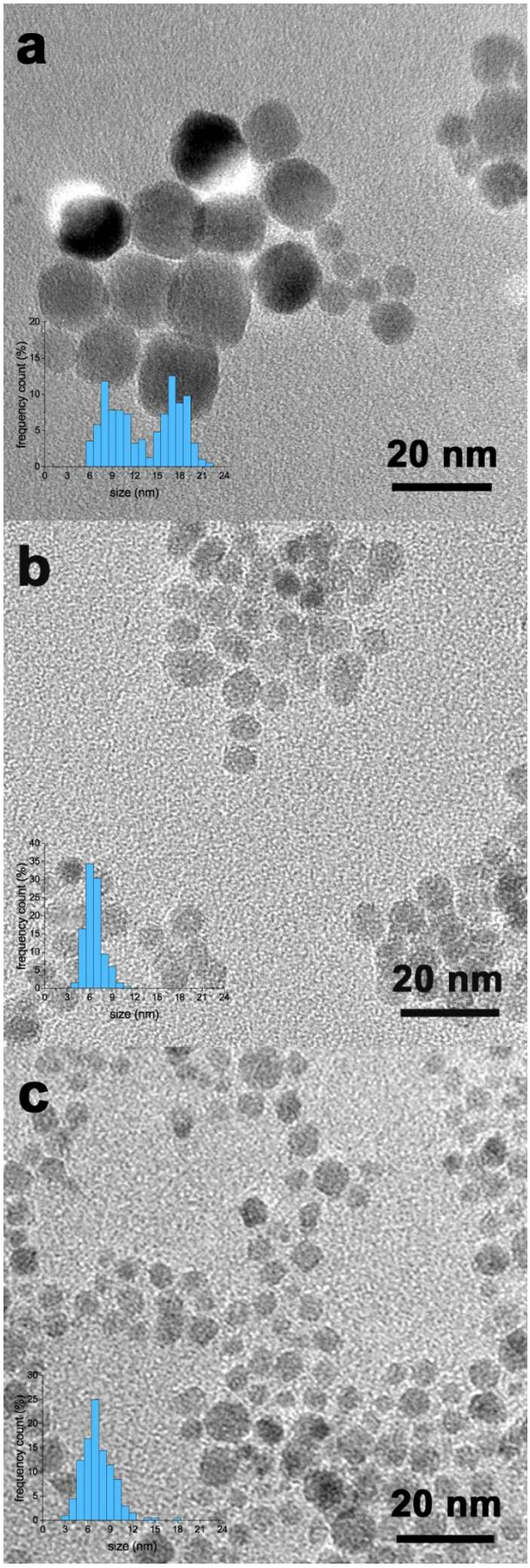

Figure 3 –TEM images of $CoFe_2O_4$ nanoparticles along with the size distribution obtained with OAm (a), OAc (b), OAc/ OAm (c)

The crystallite size distribution histogram exhibits a bimodal profile in which each of the curves fits into a lognormal distribution profile. The nanocubes have an average size of 18 nm, while the smaller particles have a size of about 8 nm. The nanoparticles obtained with OAc have not well-defined shapes, (Fig.3b), while the ones produced with OAc/ OAm (Fig.3c) have shown heterogeneous morphology, some of the particles being also cubic in shape. In both cases, the size distribution is adjusted to the lognormal distribution and the mean crystallite is 7 nm (Fig.3b and 3c). The powder synthesized with OAc has a narrower size distribution than the two other powders, indicating a greater homogeneity in crystallite size.

More details about the morphology of the particles were obtained by high-resolution transmission electron microscopy (HREM). Information about the crystalline planes coupled with the different projected shapes in the Figure 4 makes it possible to identify a cube seen along different directions. Fig.4a.b.c show the HRTEM images of $CoFe_2O_4$ particles synthesized with OAm as surfactant, respectively viewed along the $[100]$,$[10\bar{1}]$ and $[111]$ directions. The projected shape of the grain oriented along the $[100]$ is a square (Fig.4a) and he Fourier transform (FFT) (inset of Fig.4a) corresponds to the diffraction pattern along a $[100]$ zone axis of a cubic spinel structure, with the {022} and {004} planes imaged. The structure factor associated to the {200} planes is null for the spinel structure, which explains why they do not appear in the HREM image. The crystalline planes {022} and {004} are respectively at 45° and parallel to the faces (Fig. 4a), we can therefore conclude that this particle is indeed a nanocube, and not an octahedron.

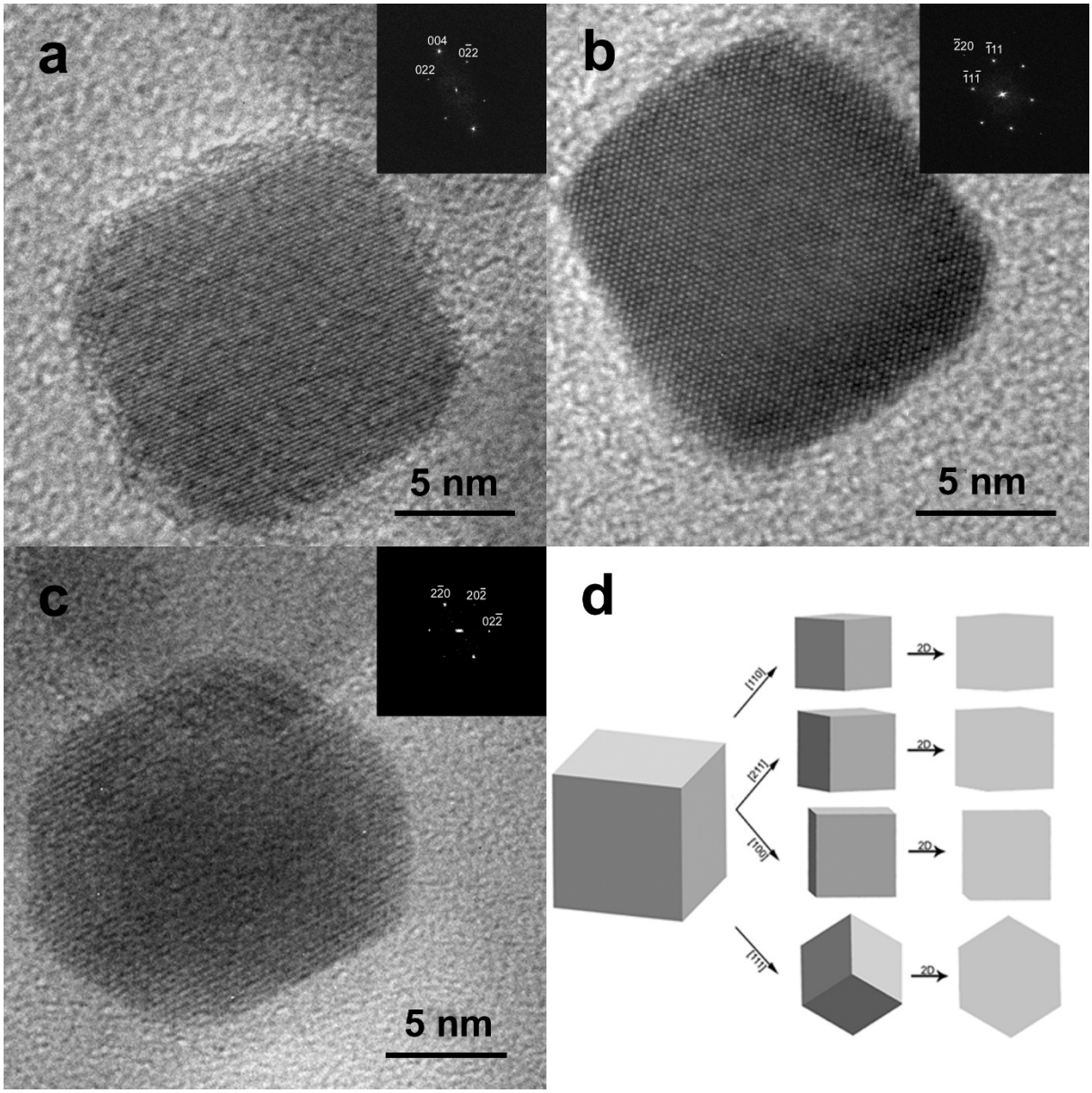

Figure 4 – HRTEM images of nanocubes of $CoFe_2O_4$ (a) oriented along [100] (b) oriented along [110] (c) oriented along [111], (d) 2D projected forms of a cube along different axes.

When the particle is oriented along $[10\bar{1}]$, the projected shape is a rectangle, and the crystalline planes imaged are {111} and {202}, the latter being parallel to one of the sides of the rectangle (Fig. 4b). For a particle oriented along a [111] direction (Fig.4c), the observed shape is hexagonal and the {220} planes of the spinel structure are parallel to the hexagon faces. For a cubic form, the projected shapes along different low index directions are shown in Fig. 4d. These projected shapes, associated with the imaging of the planes parallel to the faces, allow to conclude that Fig.4b and 4c correspond to nanocubes. The nanocubes are not always [100] oriented on the carbon grid, thus do not always exhibit a square shape. This HREM study, which

images the crystallographic planes, makes it possible to conclude that we succeeded in synthesizing nanocubes using OLA as surfactant.

Nanocubes could also be produced with the mixture of OAc/ OAm, an a typical HREM image is shown in Fig. 5a. As expected for a cube oriented along a [100] direction, the imaged crystalline planes {022} of the spinel structure are at 45° of the faces of the particles. However, these nanocubes are cobalt deficient with regards to the expected $CoFe_2O_4$ composition. Finally, using only OA as surfactant led to facetted particles (Fig.5b) with different shapes. The interaction of OAc and OAm with iron oxide nanoparticles was studied through molecular mechanics modeling [56]. It was shown that the binding energy of surfactants to the nanoparticle surfaces with OAc solely was always lower than in the case of OAc/ OAm mixtures. This may explain our results concerning the use of OAc and OAc/ OAm.

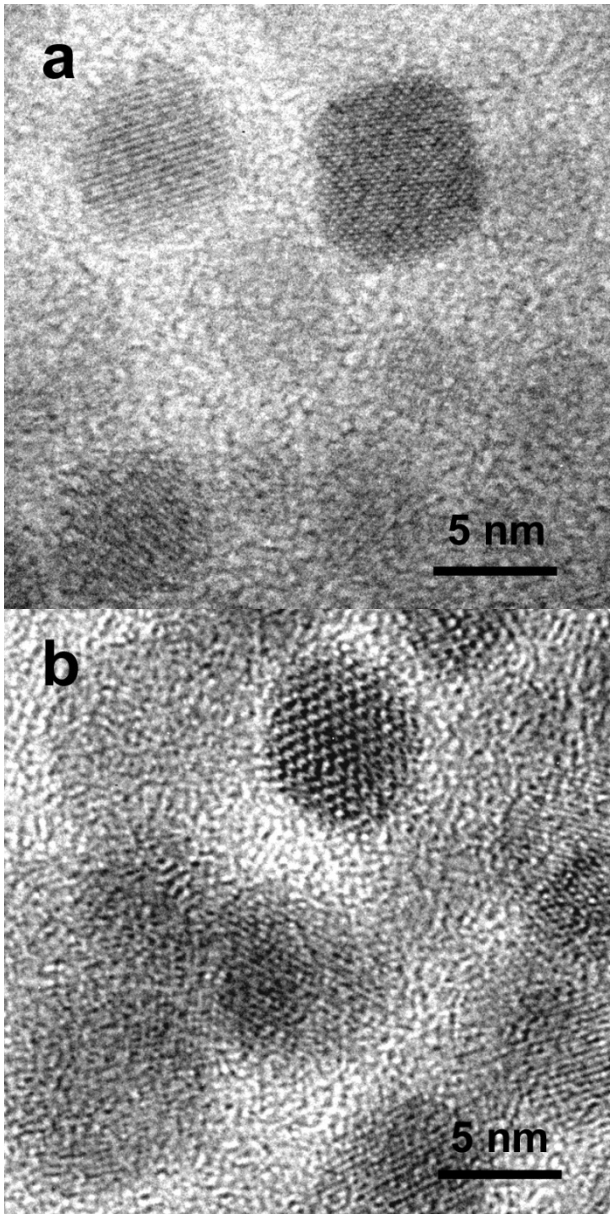

Figure 5 : a) HRTEM image of a [100] oriented $Co_{0,6}Fe_{2,4}O_4$ nanocube obtained with OAc/ OAm as surfactants, with the {220} planes imaged b) HRTEM image of a facetted $CoFe_2O_4$ particle obtained with OAc as surfactant, the {111} and {311} planes are imaged.

Influence of the amount of oleylamine on the shape and size of $CoFe_2O_4$ particles

Powders were synthesized with different amounts of OAm, characterized by a [OAm]/[Fe(acac)$_3$] ratio of 4, 5, 6, 6.5, and 7.5. Figure 6 shows the corresponding TEM images of the different powders. For [OAm]:[Fe(acac)$_3$] = 5 (Fig.6b) and 6.5 (Fig.6c), the results in terms of size and distribution are similar to those obtained with an initial ratio of 6 (Fig. 3). The $CoFe_2O_4$ nanoparticles are nanocubes of 18 nm in size and small faceted nanoparticles. For

[OAm]:[Fe(acac)$_3$] = 4 (Fig. 6a) or 7.5 (Fig.6d), there is a significant decrease in the population of nanocubes, the powders consist mainly of faceted nanoparticles without well-defined shape. This indicates that for a [OAm]: [Fe(acac)$_3$] = 4, the amount of surfactant is insufficient to influence the morphology of the particles. On the other hand, for [OAm]: [Fe(acac)$_3$] =7.5, the excess of surfactant limits the growth of the nanoparticles and leads to a powder composed mainly of small polyhedral particles [35]. Therefore, in the current study, the formation of nanocubes was observed for a ratio of [OAm] surfactant to the [Fe(acac)$_3$] precursor in the range of 5 to 6.5.

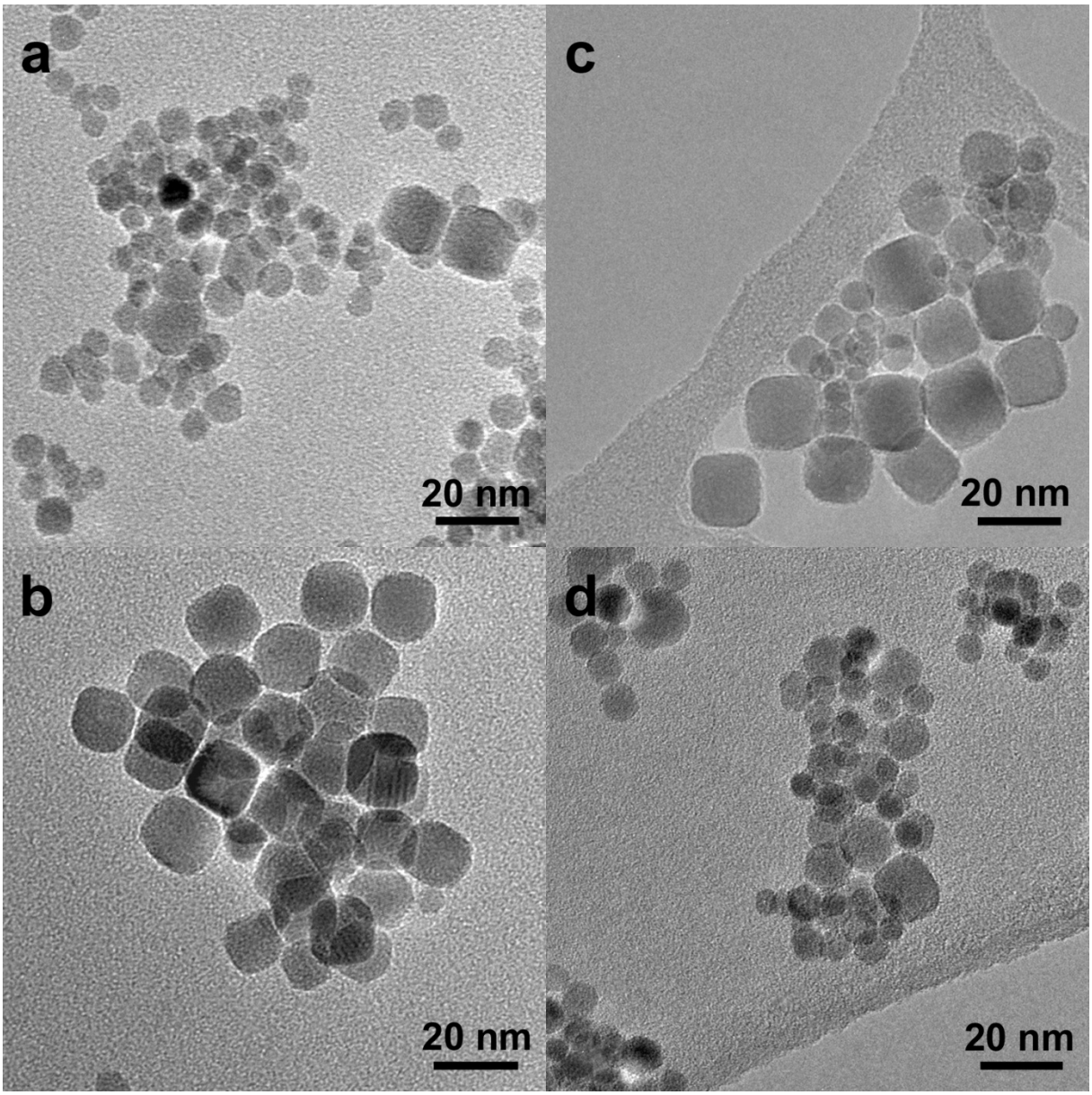

Figure 6 Effect of the concentration of oleylamine on the $CoFe_2O_4$ particle shape a) [OAm]:[$Fe(acac)_3$] = 4.0 b) [OAm]:[$Fe(acac)_3$] = 5 c) [OAm]:[$Fe(acac)_3$] = 6.5 d) [OAm]:[$Fe(acac)_3$] = 7.5

Effect of the synthesis parameters

The effect of other synthesis parameters such as the time and temperature of the solvothermal synthesis and the concentration of the precursor was also investigated. For each condition of synthesis analyzed only one of the parameters was modified.

Figure 7 shows TEM images of $CoFe_2O_4$ powders synthesized at 175 °C for different synthesis times 12h (Fig. 7a), 24h (Fig. 7b) 48h (Fig. 7c) and 96h (Fig. 7d). The size distribution for each powder is indicated. The reaction time clearly influences the size distribution of the particles. A short time of solvothermal synthesis (12h) gives a majority of faceted and small nanoparticles (8-10 nm). Some nanoparticles have a size in the range of 14 nm to 18 nm. However, despite the size approaching the size of the cubes obtained in the synthesis performed during 48h (Fig. 7c), these nanoparticles are not clearly cubes. The bimodal distribution of nanocubes and faceted nanoparticles appears for a reaction time of 24 hours. A reaction time of 48h seems to widen the size distribution of the smaller particles, and a time of 96h tends to remove the bimodal nature of the size distribution.

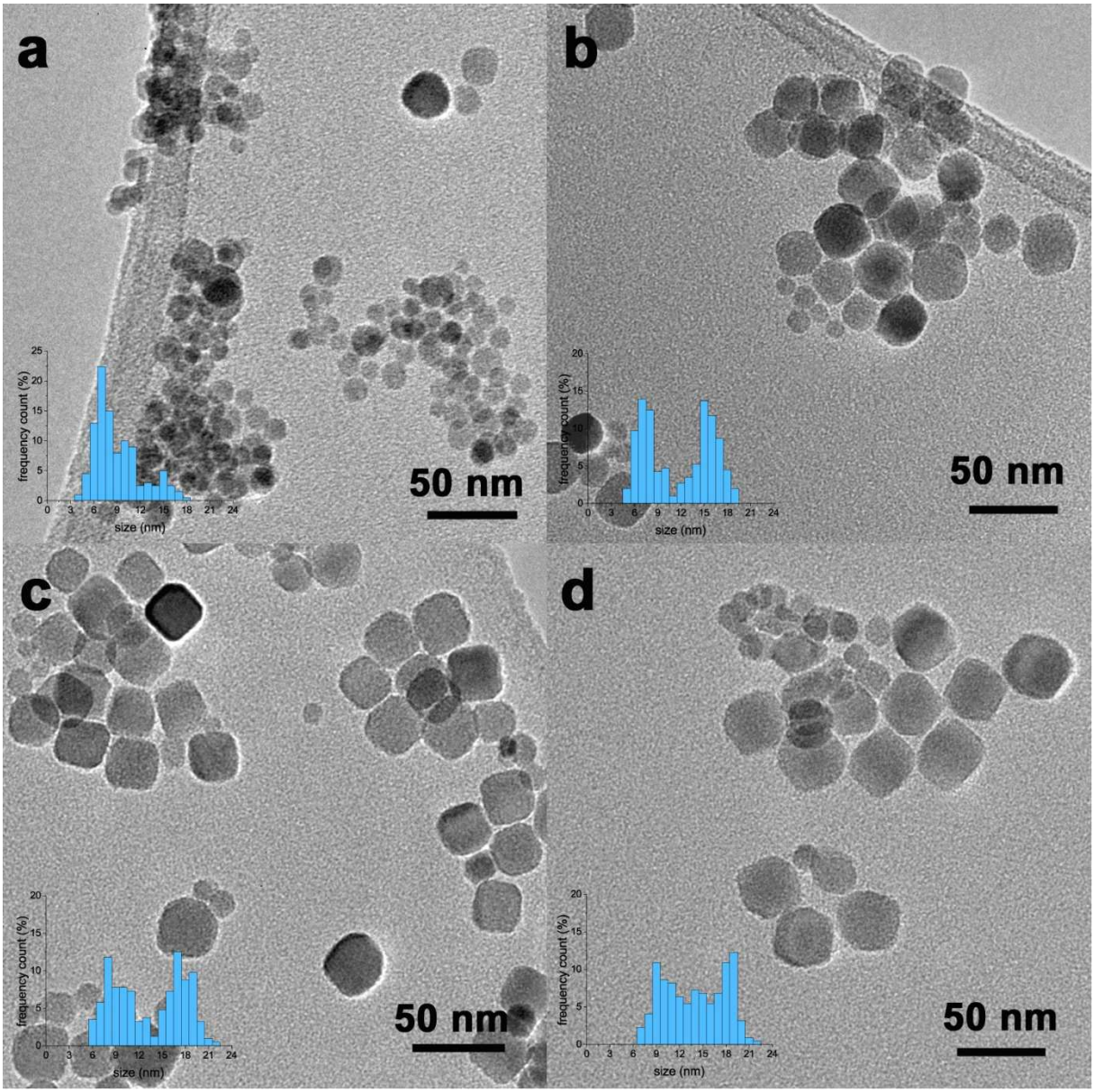

Figure 7 – $CoFe_2O_4$ nanoparticles produced at 175°C and [OAm]:[$Fe(acac)_3$] = 6 for a) 12h, b) 24h, c) 48h, d) 96h.

The temperature of the solvothermal treatment influences also the morphology of the $CoFe_2O_4$ nanoparticles. Figure 8 shows TEM images of $CoFe_2O_4$ nanoparticles along with the particle size distribution for thermal treatments at 150°C and 200 °C, during 24h. Due to the teflon nature of the vessel, temperatures above 200°C could not be tested.

The powder synthesized at 200 ° C has a bimodal size distribution (Fig. 8b) but this bimodality is less marked than in the case of the powder obtained at 175 °C for 24 hours (Fig.7b). There is an increase of both populations and a size overlap. The increase of temperature from 175ºC to 200ºC, therefore, has a similar effect to an increase of the reaction time from 48 to 96

hours (Fig.7). The small particles have intermediate forms between cubes and spheres and an average size of 9-10 nm. The largest nanocubes (16-18 nm) obtained at 200 °C appear with more rounded corners and faces than those obtained at 175 °C, indicating that an increase in temperature favors the appearance of micro facets {111} or {110}.

The powder obtained at 150 °C for 24 hours (Fig. 8a) also has two populations of particles with a weak bimodal size distribution, as in the case of the powder obtained at 200 °C. The size of the nanoparticles is smaller than in the case of other powders: the average value of the smallest particles is 7 nm and the larger ones have an average size of 12-13 nm. As in the previous cases (175 °C and 200 °C), the larger particles have a shape close to the cube whereas for the small ones the shape is not so well defined. So, a small temperature variation of ± 15 % around 175°C gives a more or less bimodal distribution.

Similar results were obtained on the synthesis of FePt nanocubes from the thermal decomposition of organometallic precursors. The formation of cubic or spherical nanoparticles is then linked to the reaction temperature, and the increase in temperature favors the production of spherical nanoparticle [44].

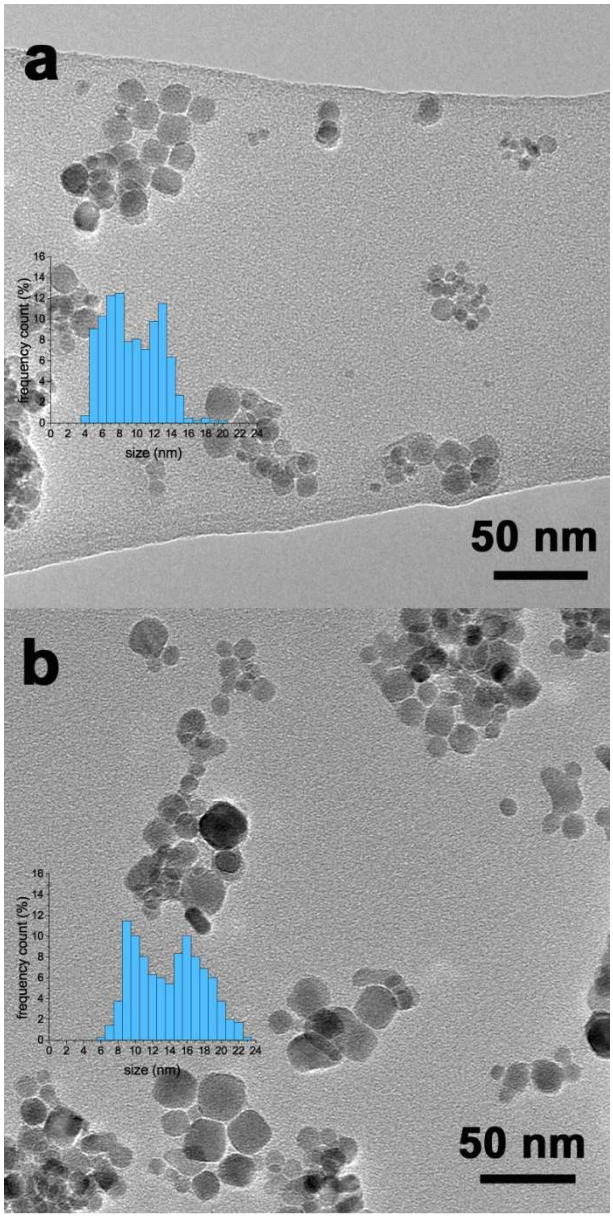

Figure 8 : $CoFe_2O_4$ nanoparticles and size distribution obtained at different temperature (a) 150ºC for 24h (b) 200ºC for 24h.

Figure 9 shows the influence of the concentration of Fe (III) and Co (II) acetylacetonates on the $CoFe_2O_4$ nanoparticles shape, in the 0.08M to 0.6M range. For precursors concentration of 0.15 M and 0.31 M, nanocubes were produced. (Fig. 9b and 9c). However, for low (0.08M) or high concentration (0.6M) only small nanoparticles without well-defined shape with average size of 7.5 and 9 nm, respectively, were obtained (Fig.9a and 9d).

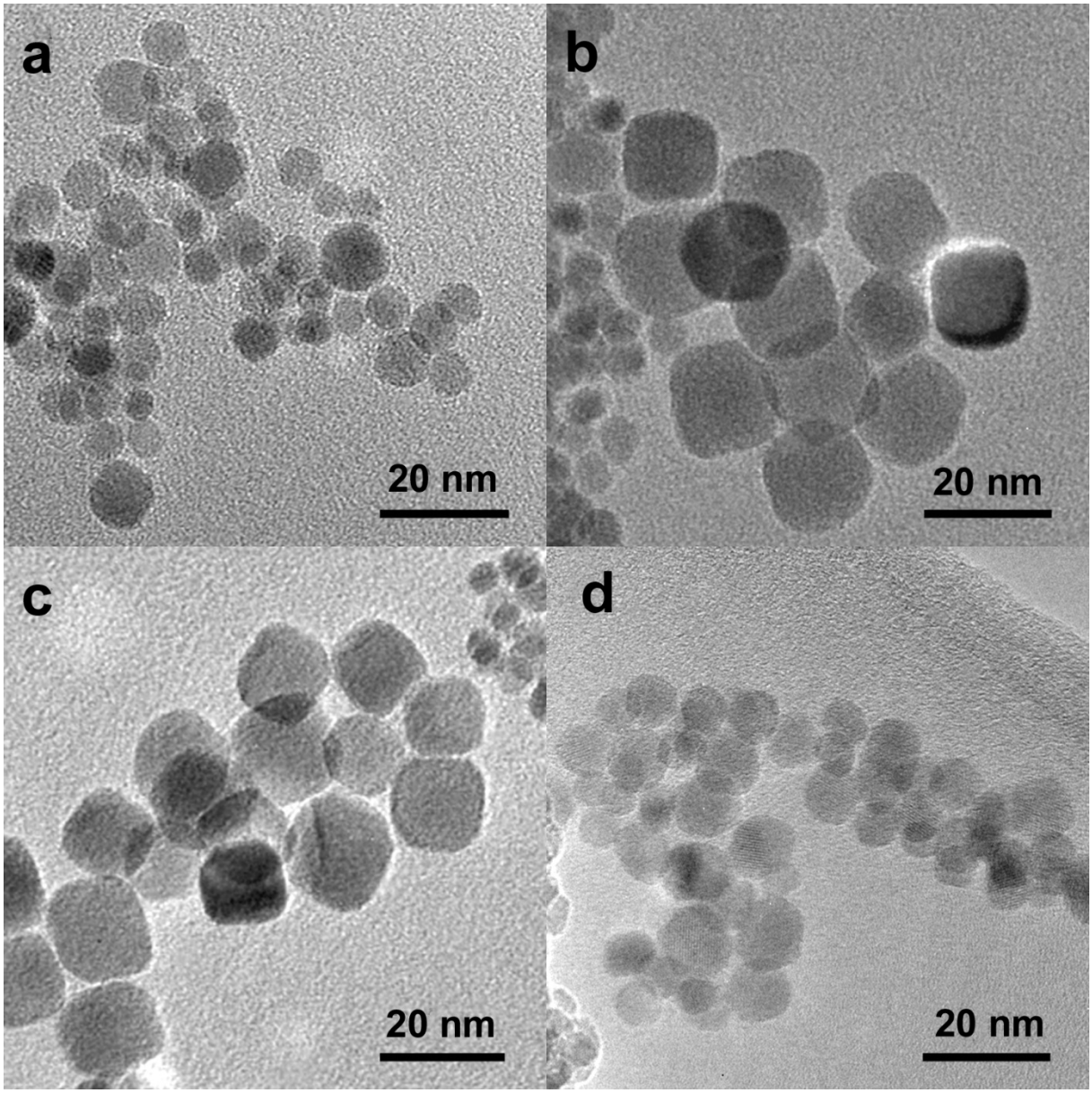

Figure 9 – $CoFe_2O_4$ nanoparticles synthesized at 175°C with different acetylacetonates concentration (a) 0.08M (b) 0.15M (c) 0.31M (d) 0.6M

A high concentration of precursors increases the rate of germs and promotes the formation of a large number of small particles, followed by their coalescence due to a proximity effect of germs. This promotes rapid particle growth, and thus comparable kinetics of the different facets leading to spherical shapes or to not well-defined shapes [61]. A too low concentration of precursors limits nuclei growth due to lack of material in their vicinity, which results in a lower rate of diffusion and collisions, favoring the formation of small particles. Hence, small particles are observed.

According to the results shown in this paper, it appears that the synthesis of nanocubes can be obtained under very specific conditions of temperature, time, nature of surfactant, as well as concentration of precursors and surfactant . Figure 10 shows a typical population of nanocubes.

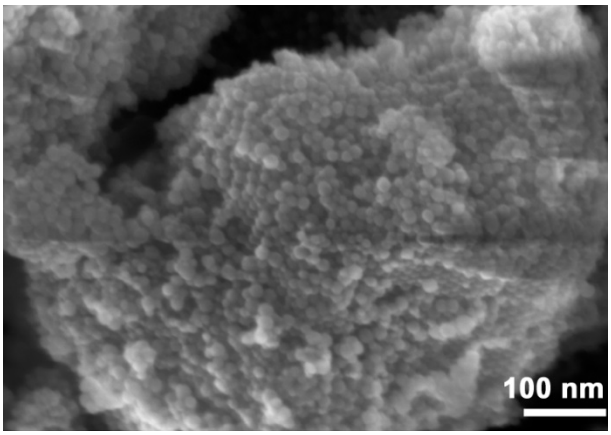

Figure 10 SEM image of $CoFe_2O_4$ nanoparticles synthesized at 175°C, with an acetylacetonate concentration of 0.15 M, and an OAm concentration of 0.6M.

Well defined nanocubes were obtained with OAm, not with OAc or a mixture of OAc/ OAm. In literature, solely OAm led to spherical nanoparticles and this was attributed to weak bonding of OAm on the surfaces of the particles [62-64]. On the contrary, the strong binding of OAc on the particles surfaces was considered to be responsible of the shape control [50,65].But then, the most used synthesis method in these papers was the thermal decomposition one. In case of a solvothermal route using benzyl alcoohol and OAm, as in this work, nanocubes of Pt were successfully grown [66]. This indicates that the shape control is not only linked to the nature of surfactant, but also to the synthesis method in which the surfactant are used. A nanocube is an out of equilibrium form, so can be obtained in out of equilibrium process when the growth velocity of {100} facets is limited, or the growth of {111} and {110} facets is increased. A possible explanation for the formation of nanocubes would be that, in the presence of OAm, during the growth process, the smaller nanoparticles coalesce preferably on a specific facet of the larger nanoparticles, ie {111} [67] and/or that the OAm molecules are adsorbed onto the cobalt ferrite facets {100}, limiting the growth of these faces. In this work, the nanocubes powders exibit a

bimodal size distribution, with nanocubes around 20 nm and smaller particles around 8 nm, a mixture of cubes and facted particles. A bimodal size distribution is often explained by the Ostwald ripening process, in which larger particles grow at the expense of smaller ones [68,69]. The fact that increasing time of synthesis from 12h to 96 h diminish the amount of small particles points to this ripening process . Bimodal nanoparticles size distribution has been already observed by other researchers in the synthesis of nanoparticles using OAm as surfactant and in the production of nanoparticles by solvotermal methode [43,68,70-71].

Conclusion

Cobalt ferrite nanoparticles were obtained from the non-aqueous route of benzyl alcohol with the addition of different surfactants. The nanoparticles synthesized with OAm have a cubic shape, with the stoichiometric composition $CoFe_2O_4$, and exhibit a bimodal size distribution.The nanoparticles synthesized with OAc solely have no specific shape, and those obtained with an equimolar mixture of OAc and OAm are cobalt deficient with a $Co_{0.6}Fe_{2.4}O_4$ composition.

The synthesis parameters (surfactant concentration, precursor concentration, temperature and reaction time) influence the shape of the nanoparticles synthesized in the presence of OAm. The different analyzed parameters did not allow to obtain one sized nanocubes, however, for the first time, stoichiometric $CoFe_2O_4$ nanocubes were obtained, using a solvothermal route with benzyl alcohol and oleylamine.

Acknowledgements

This work was done in the general framework of the CAPES COFECUB PHC 777-13 French – Brazilian cooperation project.

389

390 **References**

391 [1] N. Sanpo, J. Tharajak, Y. Li, C.C. Berndt, C. Wen, J. Wang, Biocompatibility of transition
392 metal-substituted cobalt ferrite nanoparticles, J. Nano. Res. 16 (2014) 2510.
393 https://doi.org/10.1007/s11051-014-2510-3

394 [2] A. Sunny, K.S.A. Kumar, V. Karunakaran, M. Aathira, G.R. Mutta, K.K. Maiti, V. R. Reddy, M.
395 Vasundhara, Magnetic properties of biocompatible $CoFe_2O_4$ nanoparticles using a facile
396 synthesis, Nano-Structures & Nano-Objects 16 (2018) 69–76.
397 https://doi.org/10.1016/j.nanoso.2018.04.003

398 [3] M. Amiri, M. Salavati-Niasari, A. Akbari, Magnetic nanocarriers: Evolution of spinel ferrites for
399 medical applications, Adv. Col. Inter. Sc. 265 (2019) 29–44.
400 https://doi.org/10.1016/j.cis.2019.01.003

401 [4] J. Li, D. Dai, X. Liu, Y. Lin, Y. Huang, L. Bai, Preparation and characterization of self-formed
402 $CoFe_2O_4$ ferrofluid, J. Mater. Res. 22 (2007) 886–892. https://doi.org/10.1557/jmr.2007.0134

403 [5] J. Kim , H. S. Kim , N. Lee, T. Kim, H. Kim, T. Yu , I. C. Song , W. K. Moon , T. Hyeon ,
404 Multifunctional Uniform Nanoparticles Composed of a Magnetite Nanocrystal Core and a
405 Mesoporous Silica Shell for Magnetic Resonance and Fluorescence Imaging and for Drug
406 Delivery, Ang. Chem. Int . Ed 47 (2008) 8438-8441. https://doi.org/10.1002/anie.200802469

407 [6] K.K. Kefeni, T.A.M. Msagati, B.B. Mamba, Ferrite nanoparticles: Synthesis, characterisation
408 and applications in electronic device, Mat. Sci. Eng. B. 215 (2017) 37–55.
409 https://doi.org/10.1016/j.mseb.2016.11.002

410 [7] S.Y. Srinivasan, K.M. Paknikar, D. Bodas, V. Gajbhiye, Applications of cobalt ferrite
411 nanoparticles in biomedical nanotechnology, Nanomedicine 13 (2018) 1221–1238.
412 https://doi.org/10.2217/nnm-2017-0379

413 [8] M. Vasilakaki, N. Ntallis, N. Yaacoub, G. Muscas, D. Peddis and K. N. Trohidou, Optimising
414 the magnetic performance of Co ferrite nanoparticles via organic ligand capping, Nanoscale 10
415 (2018) 21244-21253. https://doi.org/10.1039/c8nr04566f

416 [9] DS Mathew DS, RS Juang, An Overview of the Structure and Magnetism of Spinel Ferrite

417 Nanoparticles and Their Synthesis in Microemulsions, Chem. Eng. J. 129 (2007) 51-65.
418 https://doi.org/10.1016/j.cej.2006.11.001
419 [10] L. Ajroudi, N. Mliki, L. Bessais, V. Madigou, S. Villain, C. Leroux, Magnetic, electric and
420 thermal properties of cobalt ferrite nanoparticles, Mat. Res. Bull. 59 (2014) 49–58.
421 https://doi.org/10.1016/j.materresbull.2014.06.029
422 [11] B. J. Rani , M. Ravina , B. Saravanakumar , G. Ravi , V. Ganesh , S. Ravichandran, R.
423 Yuvakkumar, Ferrimagnetism in cobalt ferrite (CoFe2O4) nanoparticles, Nano-Structures &
424 Nano-Objects 14 (2018) 84–91. https://doi.org/10.1016/j.nanoso.2018.01.012
425 [12] H. Kumar Reddy, Y.-S. Yun, Spinel ferrite magnetic adsorbents: Alternative future
426 materials for water purification, Coord. Chem. Rev. 315 (2016) 90–111.
427 https://doi.org/10.1016/j.ccr.2016.01.012
428 [13] N Masunga, O. K. Mmelesi, K. K. Kefeni, B. B. Mamba, Recent advances in copper ferrite
429 nanoparticles and nanocomposites synthesis, magnetic properties and application in water
430 treatment, J. Env. Chem. Eng. 7 (2019), 103179. https://doi.org/10.1016/j.jece.2019.103179
431 [14] A. Šutka, K.A. Gross, Spinel ferrite oxide semiconductor gas sensors, Sensors and
432 Actuators.B 222 (2016) 95–105. https://doi.org/10.1016/j.snb.2015.08.027
433 [15] B.I. Kharisov, H.V.R. Dias, O. V. Kharissova, Ferrite nanoparticles in catalysis, Arab. J.
434 Chem. 270 (2014) 26723–26726. https://doi.org/10.1016/j.arabjc.2014.10.049
435 [16] P. Martins, R.Gonçalves, A.C.Lopes, E.Venkata Ramana, S.K.Mendiratta, S.Lanceros-
436 Mendez, Novel hybrid multifunctional magnetoelectric porous composite films, J.
437 Mag.Mag.Mat. (2015) 396 237-241, https://doi.org/10.1016/j.jmmm.2015.08.041
438 [17] Y. Zong, Z. Yue, P. Martins, J. Zhuang,Y. Du, S. Lanceros-Mendez and M. J. Higgins,
439 Magnetoelectric coupling in nanoscale 0–1 connectivity, Nanoscale (2018) 10 17370-17377,
440 DOI: 10.1039/c8nr05182h
441 [18] K. V. Chandekar, K. Mohan Kant, Effect of size and shape dependent anisotropy on
442 superparamagnetic property of CoFe2O4 nanoparticles and nanoplatelets, Physica B 520
443 (2017) 152–163, http://dx.doi.org/10.1016/j.physb.2017.06.001
444 [19] Q. Song, Z.J. Zhang, Shape Control and Associated Magnetic Properties of Spinel Cobalt

445 Ferrite Nanocrystals, J. Am. Chem. Soc. 126 (2004) 6164–6168
446 https://doi.org/10.1021/ja049931r
447 [20] P.S. Antonel . C. L. P. Oliveira . G. A. Jorge .O. E. Perez . A.G. Leyva . R. M. Negri
448 Synthesis and characterization of CoFe2O4 magnetic nanotubes, nanorods and nanowires.
449 Formation of magnetic structured elastomers by magnetic field-induced alignment of CoFe2O4
450 nanorods, J Nanopart Res (2015) 17:294, DOI 10.1007/s11051-015-3073-7
451 [21] Y. Kumar , A. Sharma , P. M. Shirage , Impact of different morphologies of CoFe2O4
452 nanoparticles for tuning of structural, optical and magnetic properties, J.Alloys and Compounds
453 (2019) 778 398-409 https://doi.org/10.1016/j.jallcom.2018.11.128
454 [22] H. Lee, Utilization of shape-controlled nanoparticles as catalysts with enhanced activity and
455 selectivity, RSC Adv. 4 (2014) 41017–41027. https://doi.org/10.1039/C4RA05958A
456 [23] L. Ajroudi, S. Villain, V. Madigou, N. Mliki, C. Leroux, Synthesis and microstructure of cobalt
457 ferrite nanoparticles, J. Cryst. Growth 312 (2010) 2465–2471.
458 https://doi.org/10.1016/j.jcrysgro.2010.05.024
459 [24] L. Ajroudi, V. Madigou, S. Villain, N. Mliki, and Ch. Leroux, Potentiality of Cobalt
460 Nanoferrites for Gas Sensors, Sensor Letters Vol. 9, 1–4, 2011,
461 https://doi.org/10.1166/sl.2011.1798
462 [25] Y.Tang, X.Wang, Q.Zhang, Y.Li, H.Wang, Solvothermal synthesis of Co1-xNixFe2O4
463 nanoparticles and its application in ammonia vapors detection, Prog .Nat. Sc. Mat. Int. 22
464 (2012) 53-58. https://doi.org/10.1016/j.pnsc.2011.12.009
465 [26] E. Manova, T. Tsoncheva, Cl. Estournes, D. Paneva, K. Tenchev, I. Mitov, L. Petrov,
466 Nanosized iron and iron–cobalt spinel oxides as catalysts for methanol decomposition, Appl.
467 Cata. A: General 300 (2006) 170–180. https://doi.org/10.1016/j.apcata.2005.11.005
468 [27] C.Xiangfeng, J.Dongli, G.Y. Z.Chenmou, Ethanol gas sensor based on nano-crystallines
469 prepared by hydrothermal method, Sensors and Actuators B, 120 (2006) 177-181.
470 https://doi.org/10.1016/j.snb.2006.02.008
471 [28] Ballarini, F. Cavani, S. Passeri, L. Pesaresi, A.F. Lee, K. Wilson, Phenol methylation over
472 nanoparticulate $CoFe_2O_4$ inverse spinel catalysts: The effect of morphology on catalytic

performance, Appl. Cat . A 366 (2009) 184–192. https://doi.org/10.1016/j.apcata.2009.07.003

[29] C. Wang, L. Yin, L. Zhang, D. Xiang, R. Gao, Metal Oxide Gas Sensors: Sensitivity and Influencing Factors, Sensors 10 (2010) 2088–2106. https://doi.org/10.3390/s100302088.

[30] J.-P. Jolivet, S. Cassaignon, C. Chanéac, D. Chiche, O. Durupthy, D. Portehault, Design of metal oxide nanoparticles: Control of size, shape, crystalline structure and functionalization by aqueous chemistry, Comptes Rendus Chim. 13 (2010) 40–51. https://doi.org/10.1016/j.crci.2009.09.012.

[31] A.L. Lopes-Moriyama, V. Madigou, C.P. de Souza, C. Leroux, Controlled synthesis of CoFe2O4 nano-octahedra, Powder Technol. 256 (2014) 482–489. https://doi.org/10.1016/j.powtec.2014.01.080.

[32] I.A. Fernandes de Medeiros, V. Madigou, A.L. Lopes-Moriyama, C. Pereira de Souza, C. Leroux, Morphology and composition tailoring of $Co_xFe_{3-x}O_4$ nanoparticles, J. Nano. Res. 20 (2018) 3. https://doi.org/10.1007/s11051-017-4097-y.

[33] D. Carta, M. F. Casula, A. Falqui, D. Loche, G. Mountjoy, C. Sangregorio, and A. Corrias, A Structural and Magnetic Investigation of the Inversion Degree in Ferrite Nanocrystals MFe_2O_4 (M =Mn, Co, Ni), J. Phys. Chem. C 113 (2009) 8606–8615. https://doi.org/10.1021/jp901077c

[34] S. Gyergyek, D. Makovec, A. Kodre, I. Arčon, M. Jagodič, M. Drofenik, Influence of synthesis method on structural and magnetic properties of cobalt ferrite nanoparticles, J. Nano. Res. 12 (2010) 1263–1273. https://doi.org/10.1007/s11051-009-9833-5

[35] R. Sato Turtelli, M. Atif , N. Mehmood, F. Kubel, K. Biernacka, W. Linert, R. Grössinger,Cz. Kapusta, M. Sikora, Interplay between the cation distribution and production methods in cobalt ferrite Mat. Chem. Phys. 132 (2012) 832– 838. https://doi.org/10.1016/j.matchemphys.2011.12.020

[36] J. Venturini, A. Mallmann Tonelli, T. Bender.Wermuth, R. Young Sun Zampiva, S. Arcaro, A. Da Cas Viegas,C. Pérez Bergmann, Excess of cations in the sol-gel synthesis of cobalt ferrite ($CoFe_2O_4$): A pathway to switching the inversion degree of spinels, J .Mag. Mag. Mat. 482 (2019) 1-8. https://doi.org/10.1016/j.jmmm.2019.03.057

[37] M. P. Pileni, Control of the Size and Shape of Inorganic Nanocrystals at Various Scales from Nano to Macrodomains, J. Phys. Chem. C 111 (2007) 9019-9038. https://doi.org/10.1021/jp070646e

[38] M. Bricha, Y. Belmamouni, E.M. Essassi, J.M.F. Ferreira, K. El Mabrouk, Surfactant-Assisted Hydrothermal Synthesis of Hydroxyapatite Nanopowders, J. Nanosci. Nanotech. 12 (2012) 1–8. https://doi.org/10.1166/jnn.2012.6664

[39] Z. Wu, S. Yang, W. Wu, Shape control of inorganic nanoparticles from solution, Nanoscale 8 (2016) 1237–1259. https://doi.org/10.1039/C5NR07681A.

[40] M.S. Bakshi, How Surfactants Control Crystal Growth of Nanomaterials, Cryst. Growth Des. 16 (2016) 1104–1133. https://doi.org/10.1021/acs.cgd.5b01465.

[41] Henry C., Morphology of supported nanoparticles. Prog. Surf. Sci. 80 (2005) 92–116. https://doi.org/10.1016/j.progsurf.2005.09.004

[42] Y. Xia, Y. Xiong, B. Lim, and S. E. Skrabalak, Shape-Controlled Synthesis of Metal Nanocrystals: Simple Chemistry Meets Complex Physics , Ang. Chem. Int. Ed. 48 (2009) 60 – 103. https://doi.org/ 10.1002/anie.200802248

[43] B. Bian, W. Xia, J. Du, J. Zhang, J.P. Liu, Z. Guo, A.Yan, Growth mechanisms and size control of FePt nanoparticles synthesized using Fe(CO)x (x < 5)-oleylamine and platinum(ii) acetylacetonate, Nanoscale 5 (2013) 2454-2459. https://doi.org/10.1039/c3nr33602f.

[44] B.R. Bian, J. Du, W.X. Xia, J. Zhang, J.P. Liu, W. Li,Z.Guo, A.Yan, Effect of Reaction Temperature on the Shape of FePt Nanoparticles, IEEE Trans. Magn. 50 (2014) 1–4. https://doi.org/10.1109/TMAG.2014.2322879.

[45] L. Xu, D. Liu, D. Chen, H. Liu, J. Yang, Size and shape-controlled synthesis of Rh nanoparticles, Helyon (2019) e01165 https://doi.org/10.1016/j.heliyon.2019.e01165

[46] A.I. Khan, A.V. Arasu, A review of influence of nanoparticle synthesis and geometrical parameters on thermophysical properties and stability of nanofluids, Th. Sc. Eng. Prog. 11 (2019) 334-364 https://doi.org/10.1016/j.tsep.2019.04.010

[47] D. Zhang, X. Zhang, X. Ni, J. Song, H. Zheng, Synthesis and characterization of $CoFe_2O_4$ octahedrons via an EDTA-assisted route, J. Mag. Mag. Mat. 305 (2006) 68–70.

https://doi.org/10.1016/j.jmmm.2005.11.030

[48] W. Baaziz, B.P. Pichon, Y. Liu, J.-M. Grenèche, C. Ulhaq-Bouillet, E. Terrier, et al., Tuning of Synthesis Conditions by Thermal Decomposition toward Core–Shell $Co_xFe_{1-x}O@Co_yFe_{3-y}O_4$ and $CoFe_2O_4$ Nanoparticles with Spherical and Cubic Shapes, Chem. Mater. 26 (2014) 5063–5073. https://doi.org/10.1021/cm502269s.

[49] M.P. Reddy, A.M.A. Mohamed, X.B. Zhou, S. Du, Q. Huang, A facile hydrothermal synthesis, characterization and magnetic properties of mesoporous $CoFe_2O_4$ nanospheres, J. Mag. Mag. Mat. 388 (2015) 40–44. https://doi.org/10.1016/j.jmmm.2015.04.009.

[50] L. T. Lu,N. T. Dung,L. D. Tung, C. T. Thanh, O. K. Quy, N. V. Chuc, S. Maenosono and N. T. K. Thanh, Synthesis of magnetic cobalt ferrite nanoparticles with controlled morphology, monodispersity and composition: the influence of solvent, surfactant,reductant and synthetic conditions, Nanoscale 7 (2015) 19596-19610. https://doi.org/10.1039/c5nr04266f

[51] N. Bao, L. Shen, W. An, P. Padhan, C. Heath Turner, A. Gupta, Formation Mechanism and Shape Control of Monodisperse Magnetic $CoFe_2O_4$ Nanocrystals, Chem. Mat. 21 (2009) 3458–3468. https://doi.org/10.1021/cm901033m.

[52] W. Yang, Y. Yu, L. Wang, C. Yang, H. Li, Controlled synthesis and assembly into anisotropic arrays of magnetic cobalt-substituted magnetite nanocubes, Nanoscale 7 (2015) 2877–2882. https://doi.org /10.1039/C4NR07331B

[53] A. Sathya, P. Guardia, R. Brescia, N. Silvestri, G. Pugliese, S. Nitti, I. Manna, T.Pellegrino, $Co_xFe_{3-x}O_4$ Nanocubes for Theranostic Applications: Effect of Cobalt Content and Particle Size, Chem. Mat. 28 (2016) 1769–1780. https://doi.org/10.1021/acs.chemmater.5b04780.

[54] N. Pinna, S. Grancharov, P. Beato, P. Bonville, M. Antonietti, M. Niederberger, Chem. Mater. 17 (2005) 3044-3049. https://doi.org/10.1021/cm050060+

[55] D. Li, C. Wang, D. Tripkovic, S. Sun, N.M. Markovic, V.R. Stamenkovic, Surfactant Removal for Colloidal Nanoparticles from Solution Synthesis: The Effect on Catalytic Performance, ACS Catal. 2 (2012) 1358–1362. https://doi.org/10.1021/cs300219j.

[56] U. Kurtan, H. Erdemi, A. Baykal, H. Güngüneş, Synthesis and magneto-electrical properties of MFe_2O_4 (Co, Zn) nanoparticles by oleylamine route, Ceram. Int. 42 (2016) 13350–13358.

557 https://doi.org/10.1016/j.ceramint.2016.05.046.
558 [57] L. Hu, C. De Montferrand, Y. Lalatonne, L. Motte, A. Brioude, Effect of cobalt doping
559 concentration on the crystalline structure and magnetic properties of monodisperse Co xFe 3-
560 xO 4 nanoparticles within nonpolar and aqueous solvents, J. Phys. Chem. C 116 (2012) 4349–
561 4355. https://doi.org/10.1021/jp205088x.
562 [58] S. Çınar, G. Gündüz, B. Mavis, Ü. Çolak, Synthesis of Silver Nanoparticles by Oleylamine-
563 Oleic Acid Reduction and Its Use in Making Nanocable by Coaxial Electrospinning, J. Nanosci.
564 Nanotechnol. 11 (2011) 3669–3679. https://doi.org/10.1166/jnn.2011.3812.
565 [59] Y. Yu, A. Mendoza-Garcia, B. Ning, S. Sun, Cobalt-substituted magnetite nanoparticles and
566 their assembly into ferrimagnetic nanoparticle arrays, Adv. Mater. 25 (2013) 3090–3094.
567 https://doi.org/10.1002/adma.201300595.
568 [60] R.A.Harris, P.M.Shumbula, H. van der Walt, analysis of the interaction of surfactants oleic
569 acid and oleylamine with iron oxide nanoparticles through molecular mechanics modeling,
570 Langmuir 31 (2015) 3934–3943. https://doi.org/10.1021/acs.langmuir.5b00671
571 [61] H. You, J. Fang, Particle-mediated nucleation and growth of solution-synthesized metal
572 nanocrystals: A new story beyond the LaMer curve, Nanotoday 11 (2016) 145-167.
573 https://doi.org/10.1016/j.nantod.2016.04.003.
574 [62] R. Si, Y.-W. Zhang, L.-P. You, and C.-H. Yan, rare-Earth Oxide Nanopolyhedra,
575 Nanoplates, and Nanodisks, Angew. Chem. Int. Ed. 44 (2005) 3256 –3260.
576 https://doi.org/10.1002/anie.200462573
577 [63] Z.Xu, C. Chen, Y. Hou, H.Gao and S.Sun, Oleylamine as both reducing agent and stabilizer
578 in a facile synthesis of magnetite nanoparticles, Chem. Mat. 21 (2009)1778 –1780.
579 https://doi.org/10.1021/cm.802978z
580 [64] L. Pérez-Mirabet,E. Solano,F. Martínez-Julián,R. Guzmán,J. Arbiol,T. Puig,X. Obradors,A.
581 Pomar,R. Yáñez,J. Ros,S. Ricart, One-pot synthesis of stable colloidal solutions of MFe2O4
582 nanoparticles using oleylamine as solvent and stabilizer, Mat. Res. Bul. 48 (2013) 966 –972.
583 https://doi.org/10.1016/j.materresbull.2012.11.086
584 [65] H.Yang, T.Ogawa, D.Hasegawa, M.Takahashi, Synthesis and magnetic properties of

monodisperse magnetite nanocubes, J. App.Phy. 103 (2008) 07D526. https://doi.org/10.1063/1.2833820

[66] Yi Li, Ting Bian, Jingshan Du, Yalin Xiong, Fangwei Zhan, Hui Zhang, and Deren Yang, Facile synthesis of high-quality Pt nanostructures with controlled aspect-ratio for methanol electro-oxidation, Cryst. Eng. Comm. 16 (2014) 8340-8343. https://doi.org/10.1039/C4CE00713A

[67] K.S. Sharma, R.S. Ningthoujam, A.K. Dubey, A. Chattopadhyay, S. Phapale, R.R. Juluri, et al., Synthesis and characterization of monodispersed water dispersible Fe3O4 nanoparticles and in vitro studies on human breast carcinoma cell line under hyperthermia condition, Sci. Rep. 8 (2018) 14766. https://doi.org/10.1038/s41598-018-32934-w.

[68] R.K. Wahi, Y. Liu, J.C. Falkner, V.L. Colvin, Solvothermal synthesis and characterization of anatase TiO2 nanocrystals with ultrahigh surface area, J. Col. Inter. Sci. 302 (2006) 530–536. https://doi.org/10.1016/j.jcis.2006.07.003.

[69] F.B. Effenberger, R.A. Couto, P.K. Kiyohara, G. Machado, S.H. Masunaga, R.F. Jardim, et al., Economically attractive route for the preparation of high quality magnetic nanoparticles by the thermal decomposition of iron(III) acetylacetonate, Nanotech. 28 (2017) 115603. https://doi.org/10.1088/1361-6528/aa5ab0.

[70] M. Chen, Y.-G. Feng, X. Wang, T.-C. Li, J.-Y. Zhang, D.-J. Qian, Silver Nanoparticles Capped by Oleylamine: Formation, Growth, and Self-Organization, Langmuir 23 (2007) 5296–5304. https://doi.org/10.1021/la700553d.

[71] A.-Q. Zhang, L. Zhang, L. Sui, D.-J. Qian, M. Chen, Morphology-controllable synthesis of ZnO nano-/micro- structures by a solvothermal process in ethanol solution, Cryst. Res. Technol. 48 (2013) 947–955. https://doi.org/10.1002/crat.201300143.

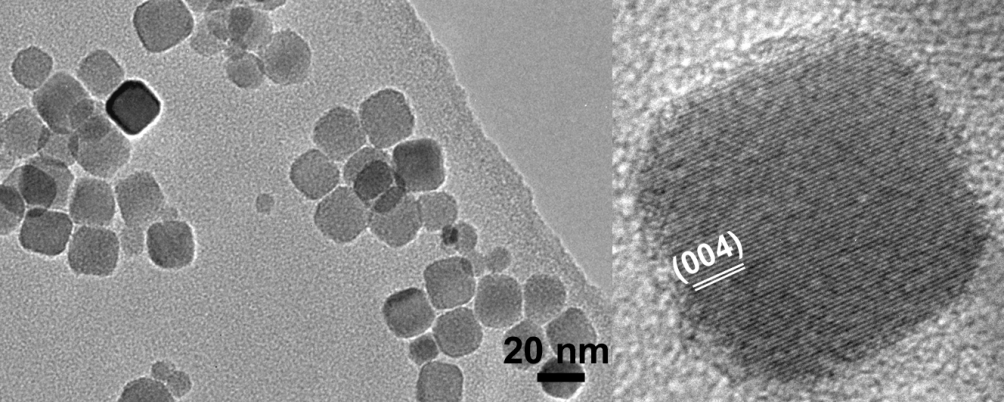
20 nm
(004)